Hydrothermal liquefaction of Spanish crude olive pomace for biofuel and biochar production

Cutz, Luis; Misar, Sarvesh; Font, Bernat; Al-Naji, Majd; de Jong, Wiebren

DOI
10.1016/j.jaap.2025.107050

Publication date
2025

Document Version
Final published version

Published in
Journal of Analytical and Applied Pyrolysis

Citation (APA)
Cutz, L., Misar, S., Font, B., Al-Naji, M., & de Jong, W. (2025). Hydrothermal liquefaction of Spanish crude olive pomace for biofuel and biochar production. *Journal of Analytical and Applied Pyrolysis*, *188*, Article 107050. https://doi.org/10.1016/j.jaap.2025.107050

Journal of Analytical and Applied Pyrolysis 188 (2025) 107050

Contents lists available at ScienceDirect

Journal of Analytical and Applied Pyrolysis

journal homepage: www.elsevier.com/locate/jaap

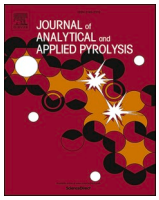

Hydrothermal liquefaction of Spanish crude olive pomace for biofuel and biochar production

Luis Cutz [a,*], Sarvesh Misar [a], Bernat Font [b], Majd Al-Naji [c], Wiebren de Jong [a]

[a] Process and Energy Department, Delft University of Technology, Leeghwaterstraat 39, Delft 2628 CB, the Netherlands
[b] Marine and Transport Technology, Delft University of Technology, Mekelweg 2, Delft 2628 CD, the Netherlands
[c] BasCat – UniCat BASF JointLab, Technische Universität Berlin, Hardenbergstraße 36, Sekr. EW K-01, Berlin 10623, Germany

ARTICLE INFO

Keywords:
Hydrothermal liquefaction
Crude olive pomace
Bio-oil
Biochar
Catalysis

ABSTRACT

The olive oil industry is an important source of agricultural residues throughout its value chain, ranging from intermediate process slurries to relatively dry content pruning residues. Among them, crude olive pomace (COP) is of particular interest since it is abundant, low cost and can be a promising source for bioenergy. Nevertheless, because COP is phytotoxic and has a high moisture content and low energy density, it represents a challenge to conventional processes that usually require a dry and homogenous material. The main novelty of this study is the use of a transition metal catalyst and a central composite design (CCD) approach to optimize the conversion of COP through hydrothermal liquefaction (HTL) into valuable products. Results show that catalytic HTL is capable of converting up to half of the COP into bio-oil. Higher process temperatures resulted in lower bio-oil yields but larger higher heating value (HHV) and lower N content. The bio-oils produced at higher temperatures also show lower concentration of phenols and regarding biochar, a low inorganic content. Without any further upgrading, COP bio-oils produced by HTL are rich in valuable compounds such as oleic acid, phenolic compounds and ketones that can be used in the polymer industry or as chemical intermediates. The highest bio-oil yield was 51.96 wt% at 330 °C for 30 min and 7.5 wt% catalyst with a HHV of 22.0 MJ/kg. At those operational conditions, the biochar yield was 16.49 wt% with a HHV of 8.9 MJ/kg. The major minerals found in the biochars (CaO, SiO_2 and P_2O_5) suggests that biochar could be well-suited for use in soil applications or as materials for adsorption, especially the non-catalytic ones. Furthermore, the experimental results acquired from HTL of COP were used to develop a global kinetic model. Using an explicit Runge-Kutta method, the kinetic parameters were calculated. After comparing the global kinetic model with a linear system of ordinary differential equations (ODEs) based on the CCD models, results indicate that this approach is more effective in predicting the yields of HTL products.

1. Introduction

In the olive industry, there are two types of pomaces: the first one resulting from the olive oil extraction stage referred as “crude olive pomace” (COP) or in Spanish, “alperujo”. The moisture content of COP ranges from 65 % to 75 % for a two-outlet process or 45 %-55 % for a three outlet process [1,2]. The difference between these two processes is that the two-outlet separators can work without adding water, preventing the reduction of phenol content in the olive oil [3]. The second type of pomace is obtained when COP is further processed in pomace extraction plants to produce COP oil, and the resulting by-product is known as “extracted olive pomace” (EOP) or in Spanish, “orujillo”. It is noteworthy that not all olive industries make further use of COP for oil extraction, hence it is estimated that more than 13 Mton of COP were discarded as process residue in 2017/2018, representing a loss of bioenergy potential [4]. COP is also known to host several bioactive compounds such as minerals, polyunsaturated fatty acids and phenolic compounds which can be used to produce high-added value products [5]. However, due to the phytotoxicity and heterogeneous composition of COP, most existing conversion technologies for COP either produce low-value byproducts (such as compost or animal feed [6]) or require expensive, environmentally harmful, and energy intensive processes to convert COP into electricity [2,5]. For example, in Spain since the late 1980s, the most common way to valorize COP has been secondary extraction of olive oil followed by combustion of the exhausted COP for electricity production [6]. This method of valorization is inefficient

* Corresponding author.
E-mail address: luis.cutz@tudelft.nl (L. Cutz).

https://doi.org/10.1016/j.jaap.2025.107050
Received 30 June 2024; Received in revised form 26 January 2025; Accepted 18 February 2025
Available online 20 February 2025

since it requires a large amount of energy to dry the COP before subsequent extraction, as well as the costs of transporting relatively moist biomass. In this regard, HTL has proven to be a suitable technology to convert feedstocks with high moisture content and heterogenous composition into higher value products [7].

HTL is a process that uses a solvent, typically water, to convert biomass into four product fractions in the presence/absence of a catalyst at temperatures ranging from 200 to 374°C and pressures between 2 and 25 MPa [8–10]. These four fractions consist of an aqueous phase, a bio-oil, a biochar, and a gaseous phase. The bio-oil obtained from HTL has similar properties as petroleum crude [11] and if upgraded it can be used as a drop-in fuel (gasoline, diesel, kerosene, heavy fuel oil) [8]. Few studies have focused on processing olive residues via HTL with no specification of the nature of the residue mixture [1,12] and few others on converting COP via HTL [13,14]. The research on olive residues [1, 12] indicate that HTL of can produce bio-oil yields of 15–31 wt% with a HHV of 26–34 MJ/kg. In contrast, the bio-oil yields for COP [14] show a range of 31–39 wt% with HHVs between 26 and 32 MJ/kg. It is important to mention that these studies [1,12,14] used a one-factor-at-a-time (OFAT) approach, which restricts the study of the relationships between different operational factors within the HTL process. For example, de Filipis et al. [1] studied the impact of a fixed temperature (320°C) and residence time (30 min) using catalysts (CaO and Zeolite) on olive residues HTL products. Evcil et al. [12] investigated how the temperature (250–330°C) and residence time (15 min) influenced the yields of bio-oil and biochar from HTL of olive waste. They also examined the influence of residence time (5–60 minutes) on the yield of bio-oil and biochar at 300°C. Furthermore, Evcil et al. [12] investigated the effect of catalysts ($AlCl_3$ and $SnCl_2$) on the yield of bio-oil and biochar from HTL of olive residues at 300°C and 15 min. Dahdouh et al. [14] studied the independent effects of dry matter/water ratio, temperature and residence time on the yields of bio-oil and biochar from HTL of COP.

To the best knowledge of the authors, no comprehensive study has been conducted to investigate the influence of operational conditions on the HTL of COP. Furthermore, to date, no studies have evaluated the impact of catalyst loading on improving both the yield and quality of the COP bio-crude produced using HTL. This work examines the relationship between several operational variables (temperature, residence time, catalyst loading) and the yields of different products obtained from HTL, both with and without catalyst. The experimental work in this study was divided into two campaigns: COP screening and Central Composite Design (CCD) campaign. The COP screening was carried out to validate the reported COP HTL methodologies and results [1,12,14]. Meanwhile, the CCD campaign used a design of experiment (DoE) approach with a Response Surface Method (RSM) to evaluate the impact of operational variables on the bio-oil yield and the interactions among different parameters. Different analytical techniques were used to analyze the COP, bio-oil, and biochar qualities obtained at different operational conditions. This study fills a significant gap in the current advancements of COP HTL and catalysis, offering valuable insights to the olive industry to harness the potential of COP as a cost-effective biofuel source. This could not only create supplementary revenue streams for the olive industry but also contribute to achieving several key Sustainable Development Goals (SDGs), such as increasing employment opportunities (SDG 1, 8) and promoting sustainable energy production (SDG 7).

2. Materials and methods

2.1. Samples of COP

Samples of COP were obtained from an olive mill in Jaén, Spain and shipped to The Netherlands. Prior to shipment, the samples were stored in N_2-flushed 5 L plastic containers. No conditioning or pre-treatment was required for COP samples before HTL testing.

2.2. HTL experimental procedure

Experiments were carried out in a 300 mL stainless-steel batch autoclave (Parr 4560 – Mini Bench Top Reactor, U.S.) at different reaction conditions for the screening and CCD campaign (Supplementary Information, Table S1). The reactor was heated by a built-in electric jacket. In the screening campaign, the residence time remained fixed at 15 min, since previous research [1,12] indicated that this operational condition yielded maximal bio-oil production for the HTL of olive residues. The reactor was loaded with a pre-weighed amount of biomass in water slurry such that a 15 % DM content was attained. This was achieved with 53 g of COP and 97 g of demineralized water. Furthermore, this biomass/water ratio has been shown to produce the highest bio-oil yields [15]. In the CCD campaign's catalytic tests, the catalyst was used at concentrations ranging from 0 wt% to 10wt% of dry biomass. Before initiating the heating process, the reactor was flushed one time with nitrogen to remove air and then pressurized to 0.14 MPa. The stirring speed was set to 150 rpm. The starting time of the HTL experiment was recorded after the reactor reached the temperature set point. The temperature and pressure were monitored using an online controller and data logger (Parr 4848 Reactor controller, U.S.). After the reaction time was completed, the heating jacket was turned off and the reactor vessel was cooled down using an ice bath. The pressure inside of the reactor was measured, and the gas was safely discharged. The reason behind this is that the focus of this paper is only on the bio-oil and biochar that are produced from HTL.

2.3. Product collection and extraction

To collect the products, the slurry from the reactor vessel was poured into a pre-weighed beaker (Fig. 1). The stirrer and the reactor vessel were scraped and rinsed with 35 mL of Dichloromethane (DCM, Sigma-Aldrich 99.8 % purity) to extract as much content as possible. DCM was chosen because of its low boiling point, non-polarity, and solvent efficiency, making it perfect for extracting bio-oil or other hydrocarbons from HTL [9,10]. Furthermore, due to its volatility, DCM can be removed post-extraction, leaving the desired products. After rinsing, this phase was added to the pre-weighed beaker with the slurry. Subsequently, the slurry was vacuum filtrated using a Büchner funnel with a 2.5-μm pore size filter paper (Whatman Grade 5). 15 mL of DCM were used to rinse the beaker with the slurry during filtration. The filter cake was thoroughly washed with 20 mL DCM until there was a change of color. Then, the filter cake was identified as biochar and dried in an oven (Furnace Nabertherm 30–3000 °C, Germany) at 105 °C for 24 h. This in agreement with previous protocols for HTL [1,9,10]. After drying, the biochar was weighted and stored in a desiccator for subsequent analyses.

The filtrate from vacuum filtration is a mixture of bio-oil, aqueous phase, water and DCM. In order to extract the bio-oil from this mixture, a liquid-liquid extraction was performed using DCM as the extracting solvent. The extraction was performed until there was no apparent DCM-bio-oil in the separatory funnel (15 mL of DCM in total). The DCM was later on removed from the bio-oil fraction by evaporation in a rotary evaporator (Heidolph-VAP® Precision, Heildoph Instruments, Germany) at 675 torr. The water from the aqueous phase was also removed using a rotary evaporator. Both bio-oil and aqueous phases were stored in a fridge at 4 °C until further characterization. The amount of the gaseous phase was calculated by difference.

2.4. Screening campaign for COP HTL

An OAFT was used to evaluate the influence of temperature (250°C, 270°C, 300°C, 330°C and 340°C) on the bio-oil yield, with a residence time of 15 min. This in order to compare our method with existing studies on HTL of COP or olive residues [1,12,14] and set the boundaries for the CCD campaign. HTL experiments were carried out in duplicates to ensure the accuracy of the results.

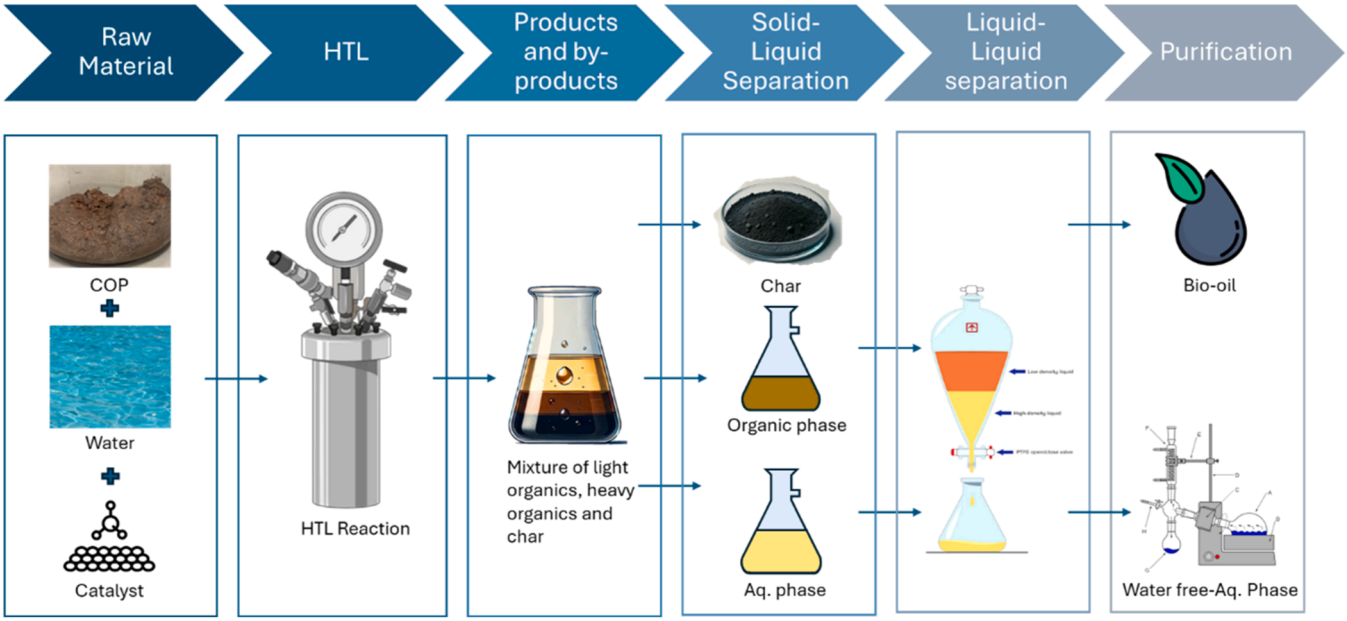

Fig. 1. HTL experimental procedure and product separation.

2.5. Central Composite Design (CCD) for COP HTL

The CCD campaign used an DoE with 3 factors: temperature (A), residence time (B), and catalyst loading (C). The design framework consists of 20 experiments containing 14 axial points and 1 center point with 6 replicates to ensure the accuracy of the model and experiments. Table 1 shows the selected factors and their corresponding levels for the CCD campaign:

The range of reaction temperature was 250 −340 °C, residence time was 5 −60 min and catalyst loading was 0 −10 wt%. The Design expert Software® version 7 was used to create the CCD. The summary of the CCD tests can be found in the Supplementary Information - Table S1. The experimental CCD results were fitted to a quadratic model indicated in Eq. (1).

$$Y = a_o + \sum_{i=1}^{3} a_i X_i + \sum_{i=1}^{3} a_{ii} X_i^2 + \sum_{i=1}^{3} \sum_{i<j} a_{ij} X_i \quad X_j \tag{1}$$

Where Y is the response function, and X_1, X_2, and X_3 are reaction temperature, residence duration, and catalyst loading, respectively. a_o is the model's intercept, and a_i, a_{ii}, and a_{ij} are the linear, quadratic, and interaction term coefficients. The accuracy of each model for each HTL fraction was assessed using the coefficient of determination (R^2), F-value, and standard error of regression (SER), sourced from the Design expert® software. The p-value was used to evaluate the statistical significance of each model.

2.6. Kinetic model and ODE system based on the CCD for HTL of COP

A global kinetic model (Fig. 2) was developed using a universal reaction network proposed by Wang et. al [16]. The data obtained from the CCD for HTL of COP was used as input for developing the kinetic model.

Table 1
Selected factors and their corresponding levels for the CCD campaign.

Factors	Levels of Factors				
	-1.633	-1	0	1	1.633
Temperature (°C)	250	270	300	330	340
Residence Time (min.)	5	10	15	30	60
Catalyst Loading (wt%)	0	2.5	5	7.5	10

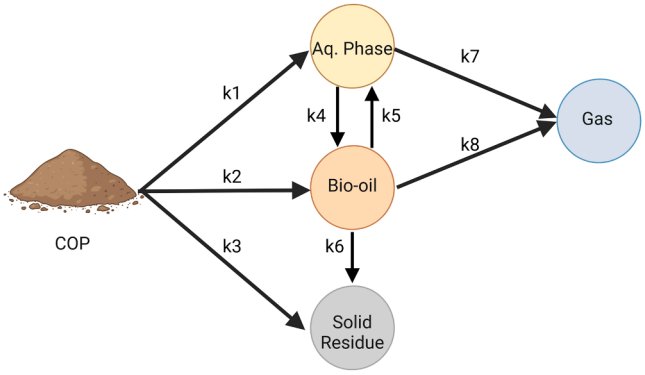

Fig. 2. Reaction network for HTL of lignocellulosic feedstocks proposed by Wang et al. [16].

$$\frac{dX_{feed}}{dt} = -(k_1 + k_2 + k_3)X_{feed} \tag{2}$$

$$\frac{dX_{AP}}{dt} = k_1 X_{feed} + k_5 X_{bio-oil} - (k_4 + k_7)X_{AP} \tag{3}$$

$$\frac{dX_{bio-oil}}{dt} = k_2 X_{feed} + k_4 X_{AP} - (k_5 + k_6 + k_8)X_{bio-oil} \tag{4}$$

$$\frac{dX_{SR}}{dt} = k_3 X_{feed} + k_6 X_{bio-oil} \tag{5}$$

$$\frac{dX_{gas}}{dt} = k_7 X_{AP} + k_8 X_{bio-oil} \tag{6}$$

Where X_{feed}, X_{AP}, $X_{bio\text{-}oil}$, X_{SR} *and* X_{gas} refer to mass fraction of COP, aqueous phase, bio-oil, solid residue (biochar) and gas, respectively. The kinetic parameters were determined by solving the system of ordinary differential equations (ODEs) using an explicit Runge-Kutta method with a relative tolerance of 1e-8 and a time-step of 0.06. The activation energy (E_a) and pre-exponential factor (A) for each k were calculated using the Arrhenius equation (Eq. 7).

$$k = A\exp\left(\frac{-E_a}{RT}\right) \tag{7}$$

The different yields from COP HTL can be analytically determined by solving a linear system of ODEs using the quadratic response function that was generated from the CCD method (Eq. 1). The linear system of ODEs provides the yields for the different HTL fractions (with respect to the residence time, t) for a given temperature (T) and catalyst loading (C). In contrast to the approach taken by Wang et. al [16], no reaction network is assumed since the ODEs system coefficients can be directly computed from the CCD RSM when considering first-order linear equations. A quadratic yield function is obtained by setting the temperature and the catalyst load.

$$Y_k(t;T,C) = a_k t^2 + b_k t + c_k = \begin{bmatrix} a_1 & b_1 & c_1 \\ \vdots & \vdots & \vdots \\ a_4 & b_4 & c_4 \end{bmatrix} \begin{bmatrix} t^2 \\ t \\ 1 \end{bmatrix} = A \begin{bmatrix} t^2 \\ t \\ 1 \end{bmatrix} \tag{8}$$

Where k is the index for the 4 different HTL fractions. As a result, the following system of linear ODEs can be derived

$$\frac{dY_k}{dt} = A\begin{bmatrix} 2t \\ 1 \\ 0 \end{bmatrix} = A\begin{bmatrix} 0 & 2 & 0 \\ 0 & 0 & 1 \\ 0 & 0 & 0 \end{bmatrix}\begin{bmatrix} t^2 \\ t \\ 1 \end{bmatrix} = A\begin{bmatrix} 0 & 2 & 0 \\ 0 & 0 & 1 \\ 0 & 0 & 0 \end{bmatrix} A^{-1} Y_k = ABA^{-1} Y_k \tag{9}$$

The ODEs system coefficients can be represented as $D = ABA^{-1}$. Taking into account the 4 HTL fractions, A is a 4×3 rectangular matrix, hence a pseudo-inverse method is employed to calculate A^{-1}. The reason for this is that the RSM is quadratic (Eq. 1), resulting in a 3×3 matrix. But since the method produces four separate ODEs, one for every fraction, the system ends up being overdetermined. The most accurate fit (least squares) is obtained using the pseudo-inverse approach, and the surface response output for the given temperature and catalyst loading is obtained by solving the ODEs system using an explicit Runge-Kutta method.

2.7. Product analysis

2.7.1. Proximate and ultimate analysis of raw COP, bio-oil and biochar

The CHNS elemental analysis of raw COP, bio-oil and biochar was conducted using a EuroVector EA3400 Series CHN-O analyzer using acetanilide as reference material. The oxygen content was determined by difference. The proximate analysis for raw COP and biochar was performed in accordance with NREL/TP-510–42621 [17], NREL/TP-510–4262 [18] and Del Grosso et al. [19]. The moisture content was determined by drying the samples at 105 °C overnight in a convection drying oven (Furnace Nabertherm 30–3000 °C, Germany) and weighed after cooling. The ash content was determined using a Muffle Furnace (FisherThermo Scientific F6030CM-33-AVL, U.S.) by incineration of the dried samples at 550 °C. The volatile matter was obtained with a thermogravimetric analyzer (TGA SDT-Q600, U.S.) by measuring the mass difference after heating the dried biomass to 600°C under nitrogen conditions and maintaining it for 10 min. All measurements for the proximate and ultimate analysis were carried out in duplicate.

2.7.2. Analytical techniques for analysis of bio-oil, biochar and aqueous phase

The HHV of the raw COP, bio-oil and biochar was determined using a Bomb Calorimeter (Parr 6772, U.S.). All measurements for the HHV were carried out in duplicate. Gas Chromatography coupled with Mass Spectrometry (GC-MS) was used to analyze the bio-oil produced from HTL at different operational conditions. The samples for GC-MS analysis were prepared by diluting the bio-oil with 2-propanol (VWR Chemicals) on a 1:10 mass ratio. Then, this fraction was filtered using a syringe 0.2 μ PTFE filter (Whatman Puradisc 13). The GC-MS was carried out using an Agilent 8890 gas chromatograph (Agilent Technologies, Wilmington, USA) equipped with an HP-5MS Ultra Inert column from Agilent (model: USR577054H), a split-splittles liner (Agilent 5190–2295) and coupled with both mass spectrometer detector. The measurement is performed by injecting the same sample three times. For more information on the detailed method for GC-MS, please refer to [20]. For compounds with a quality level above 85 %, principal component analysis (PCA) with prior normalization was applied to the peak areas of the extracted ion chromatograms. The compounds were categorized into 10 distinct classes: alcohols, benzenediols, carboxylic acids, cyclic oxygenates, esters, fatty acids, hydrocarbons, nitrogen-containing compounds, phenolics and phenones. Inductively Coupled Plasma - Optical Emission Spectrometry (ICP-OES) was used to determine the elemental concentrations in the biochar and aqueous phase of HTL. These samples were prepared by digesting approximately 0.1 g solid in demi water and aqua regia. Elemental composition data was collected utilizing a Spectro-Arcos EOP (SPECTRO Analytical Instruments GmbH, Germany) in conjunction with Spectro Smart Analyzer Vision software. In order to determine the chemical oxygen demand (COD) of the aqueous phase, a test kit (TNTplus®824, Hach) with a range between 5 and 60 g/L was used. To assess the results of the kit, the Hach test method 10212 was employed. Every sample was measured in duplicate.

3. Results

3.1. Screening campaign: effect of temperature on HTL products

Fig. 3 summarizes the results from HTL of COP at different temperatures for a residence time of 15 min. The yields for the different HTL products are expressed as mass yields (wt%).

As shown in Fig. 3, the bio-oil production increases with temperature until reaching an optimum average yield of 29 wt% at 330 °C. This is in agreement with trends reported in literature [12] for HTL of a mix of olive residues for a residence time of 15 min. Unlike findings reported in Evcil et al., [12], which identified the optimum bio-oil yield at 300 °C, the results shown in Fig. 3 demonstrate that COP's highest bio-oil yield is obtained at 330 °C. This is attributed to differences in the nature and origin of the feedstock. According to the work by Evcil et al., [12], at 330 °C for 15 min, the bio-oil yield was 28.6 wt% and the biochar yield was 22.6 wt%. At the same conditions (330 °C for 15 min), our results indicated a slightly higher bio-oil yield of 29.0 wt% and a slightly higher biochar yield of 27.6 wt%. At 340 °C, there is a decrease of 20 % in the average yield of COP bio-oil. The decrease in the bio-oil yield at 340 °C is mainly attributed to thermal decomposition and repolymerization process. This agrees with the fact that the average gas yield increased by 32 % when compared to the 330 °C point. With respect to the biochar, the yield showed a decrease with higher temperatures. This is because, particularly at high temperatures, the organic compounds in the COP underwent substantial breakdown, moving to either the gas or aqueous phase.

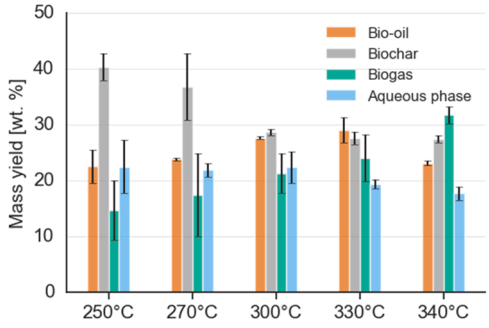

Fig. 3. Product distribution for COP HTL at different temperatures for a residence time of 15 min. The error bars represent the standard deviation.

3.2. Screening campaign: ultimate and proximate analysis of bio-oil and biochar

Table 2 and Table 3 presents the proximate and ultimate analysis of bio-oil and biochar at different temperatures for a fixed residence time of 15 min.

Based on the proximate analysis, the raw COP has a moisture content (MC) of 57.2 %, which makes it an ideal feedstock for processing through HTL. Furthermore, this result is consistent with the findings reported in literature [21], where the MC of COP ranges between 45 % and 70 % depending on the production phase. On the other hand, the ash content of the raw COP (3.6 %) was slightly lower than the value range reported in literature, 5–7 % [5,22]. In relation to the biochar produced from non-catalytic experiments (Table 2), the samples treated at different temperatures exhibited a higher ash content compared to the raw COP. This is due to the removal of volatile organic compounds and the presence of inorganic minerals in the biochar [23]. As the process temperature increased (Table 3), the volatile matter (VM) in the biochar decreased until 330°C, with a significant increase at 340°C. Higher temperatures during non-catalytic HTL resulted in a significant increase in the fixed carbon (FC) content of the biochar. This suggests an enhancement in both the quality and mass yield of the biochar, as shown in Fig. 3.

It can be seen that after the non-catalytic HTL, the bio-oil and biochar fractions exhibit a higher C-content when compared to the raw feedstock (Table 2 and Table 3). The C-content of the bio-oil and biochar increased with an increase in temperature up to 69.5 % and 75.4 %, respectively. All the biochars produced from COP HTL fall within the range reported by [12,14] for non-catalytic HTL, except for the 340°C biochar, which is the highest C-content biochar reported in literature for olive residues and COP. Unlike findings reported in [12], the hydrogen content of the bio-oil decreased as the temperature increased from 250 to 340°C (Table 2), suggesting the formation of more aromatic compounds due to deoxygenation reactions such as decarboxylation and hydrodeoxygenation [1,24]. The bio-oil and biochar had the highest S content (<0.4 %) at lower temperatures, but the lowest S content at higher temperatures. The increase in temperature led to a decline in the oxygen content levels of both bio-oil and biochar samples, primarily due to decarboxylation and dehydration reactions that took place during HTL [25].

3.3. Screening campaign: effect of temperature on HHV of bio-oil and biochar

The HHV of the obtained bio-oil and biochar fractions at different temperatures for a residence time of 15 min is presented in Fig. 4.

The average HHV of the non-catalytic bio-oil shows a gradual increase as temperature rises, peaking at a maximum of 32 MJ/kg at 340°C−15 min. The data presented in Table 2 support these findings, indicating that the bio-oil produced at 340°C had a slightly lower O/C and H/C ratio compared to the other bio-oils. In relation to the non-catalytic biochar, the higher temperature led to a slight increase in the HHV as well, except for 300°C−15 min. The maximum HHV for the biochar is obtained at 340°C−15 min, 29.2 MJ/kg. The results presented in Fig. 4 are in agreement with previous studies [12,14] on non-catalytic HTL. However, the HHVs of bio-oil and biochar obtained at 340 °C are slightly higher (1.1 % and 0.4 % respectively) compared to the non-catalytic conditions mentioned in Evcil et al. [12] for the same residence time.

3.4. Screening campaign: GC-MS of bio-oils

Fig. 5 presents the GC-MS analyses of all bio-oils produced from the HTL process for a residence time of 15 min. Table S2 in the Supplementary Information provides a detailed identification of the components in each bio-oil shown in Fig. 5.

COP is known to be highly rich in hydroxytyrosol, tyrosol, *p*-coumaric and vanillic acid [21]. Nonetheless, these compounds were not found in the COP bio-oils, except for a minor amount of vanillic acid in the form of vanillin. Hydroxytyrosol is reported to completely decompose at 220°C [26], while vanillic acid can be converted to vanillin through decarboxylation reactions occurred during HTL. From Fig. 5 it can be observed that the bio-oils have five main classes of compounds: fatty acids (oleic acid and palmitic acid), phenolic compounds (Phenol, 2-methoxy-, Phenol, 2,6-dimethoxy-, phenol, creosol), aldehydes (furfural, vanillin), ketones (2-Cyclopenten-1-one, 2-methyl-, 2,5-Hexanedione) and phthalates (Bis(2-ethylhexyl) phthalate). The high content of oxygenated compounds such as oleic acid is common in olive pomaces, and it is attributed to the lipid content in the COP [27]. The presence of oxygenated compounds is consistent with the results of the ultimate analysis (Table 2). Furthermore, COP bio-oil has a high concentration of phenolic compounds since COP naturally contains a high concentration of stable phenols. It is estimated that after olive oil extraction, 98–99 % of the phenolic compounds are in the pomace or in the olive oil mill waste water [21]. The non-catalytic bio-oil with the highest quantity of phenolic compounds is the one produced at 300 °C. Furthermore, results from GC-MS indicate that the fatty acids and ketones in the bio-oils increased proportionally with temperature. Minor compounds found in the bio-oils are aromatic compounds (Pyridine, 3-ethyl-) and alcohols (Homovanillyl alcohol). The GC-MS results reveal, however, that at 330 °C, neither aldehydes nor homovanillyl alcohol are detectable.

3.5. CCD campaign: HTL product distribution

Fig. 6 shows the yields of the CCD campaign for each of the HTL products at different temperatures, residence times and catalyst loading. The plot is derived from a second-degree polynomial that was constructed after completing the CCD experimental campaign. The quadratic models for each of the different HTL fractions are provided in Table 4. Detailed statistics for each of these models are provided in Supplementary Information, Tables S3-S10.

As can be seen from Fig. 6, the mass yield of bio-oil was greatly affected by both temperature and catalyst loading. The highest yield of

Table 2
Proximate and ultimate analysis of COP bio-oil at different operational conditions.

	Proximate analysis (wt% a.r.)				Ultimate analysis (wt% d.b.)							
	MC (%)	VM (%)	FC (%)	Ash (%)	C	H	N	S	O[a]	O/C	H/C	C/N
Raw COP	57.2	24.4	14.8	3.6	50.0	6.5	1.5	0.0	42.0	1	1.5	38.9
Bio-oil												
250°C	-	-	-	-	62.5	10.5	0.0	0.2	26.8	0.3	2.0	-
270°C	-	-	-	-	64.0	9.7	0.1	0.1	26.1	0.3	1.8	746.6
300°C	-	-	-	-	66.3	9.2	0.2	0.1	24.2	0.3	1.7	386.7
330°C	-	-	-	-	67.8	9.0	0.4	0.0	22.8	0.3	1.6	197.7
340°C	-	-	-	-	69.5	8.7	0.4	0.0	21.4	0.2	1.5	202.7

[a] by difference.

Table 3
Proximate and ultimate analysis of COP biochar at different operational conditions.

	Proximate analysis (wt% d.b.)				Ultimate analysis (wt% d.a.f.)							
Biochar	MC (%)	VM (%)	FC (%)	Ash (%)	C	H	N	S	O[a]	O/C	H/C	C/N
250°C	-	52.5	45.5	2.0	65.9	5.7	1.0	0.4	26.9	0.3	1.0	75.4
270°C	-	46.5	47.3	6.2	74.5	6.1	1.1	0.2	18.1	0.3	1.0	81.5
300°C	-	39.5	53.9	6.6	77.6	5.8	1.2	0.1	15.3	0.2	0.9	76.9
330°C	-	36.1	58.6	5.3	77.3	5.7	1.3	0.1	15.6	0.2	0.9	71.2
340°C	-	39.2	55.4	5.4	79.7	5.8	1.3	0.1	13.1	0.2	0.9	73.3

[a] by difference.

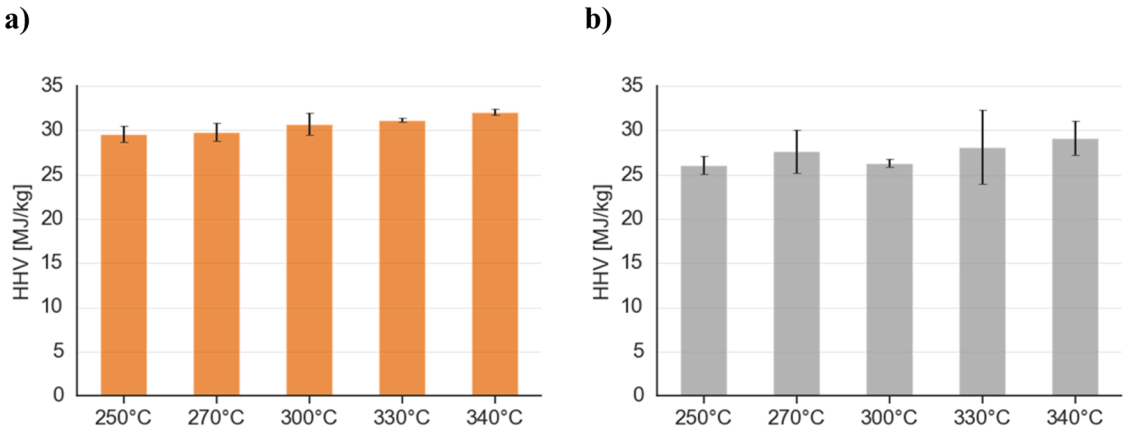

Fig. 4. High heating value (HHV) of COP a) bio-oil and b) biochar at different temperatures for a residence time of 15 min. The error bars represent the standard deviation.

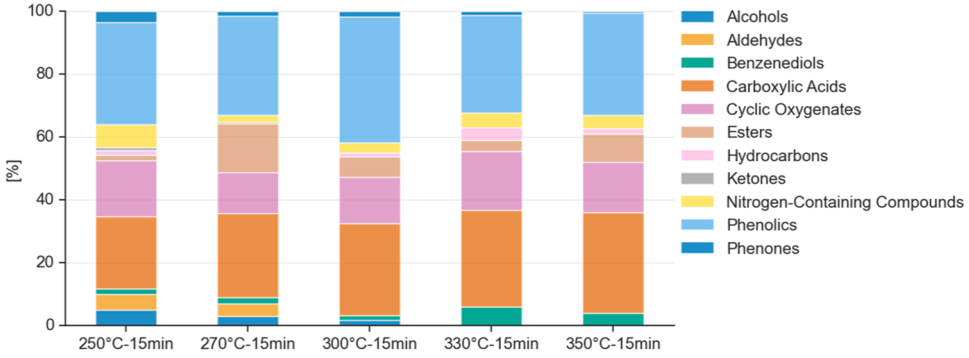

Fig. 5. GC-MS analysis for all bio-oils produced via HTL at 15 min. The figure also displays the major compounds identified in the obtained bio-oils. Detailed identification of the components in each bio-oil in Fig. 5 is provided in the Supplementary Information Table S2.

bio-oil achieved during the CCD experimental campaign was 51.96 wt% at 330°C, 30 min, and catalyst loading of 7.5 wt%. Based on the existing literature [1,12,14], this is the largest bio-yield ever reported for HTL of COP and olive oil residues. This is because Ni/SiO_2-Al_2O_3 prevents re-polymerization reactions, which reduces the production of char and lighter water-soluble and gaseous compounds [28]. Additionally, it helps break down C-C bonds in organic compounds more effectively than other catalysts [9,29].

The bio-oil yield reached its minimum value of 22.58 wt% when the reaction conditions were set at 250°C, 15 minutes, and 5 wt% catalyst concentration. The results of the non-catalytic campaign at 250°C and 15 min (22.54 ± 0.22) were comparable to this point, indicating that the Ni/SiO_2-Al_2O_3 catalyst is not the sole factor promoting high bio-oil yields. The bio-oil model was found to be statistically significant (R^2 = 0.95, F-value = 23.98 and p-value < 0.0001, Table S3 and Table S4). The model suggests that a combination of high temperature, long residence time, and a high catalyst loading will result in the best bio-oil output, 59.8 wt% with a relative error of 8 %. With respect to biochar, the yields ranged from 6.8 to 40.0 wt%. The highest biochar yield was achieved at 250°C, 15 minutes, and 5 wt% catalyst loading, whereas the lowest yield was produced at 300°C, 5 minutes, and 5 wt% catalyst loading. The biochar model demonstrated statistical significance with an R^2 value of 0.78, an F-value of 4, and a p-value of 0.0207, as shown in Table S5 and Table S6. The yields of the aqueous phase ranged from 15.5 to 26.4 wt%. The maximum yield of the aqueous phase was achieved at a temperature of 250°C, a reaction time of 15 minutes, and a catalyst loading of 5 wt%. On the other hand, the minimum yield was observed at a temperature of 330°C, a reaction time of 10 minutes, and a catalyst loading of 7.5 wt%. The aqueous phase model was found to be statistically significant (R^2 = 0.96, F-value = 29.51 and p-value < 0.0001, Table S7 and Table S8). The gas phase model was the sole surface response model that did not show statistical significance, with an R^2 value of 0.56, an F-value of 1.43, and a p-value of 0.2923 (Table S9 and Table S10). The gas phase yields ranged between 10.6 and 29.2 wt%.

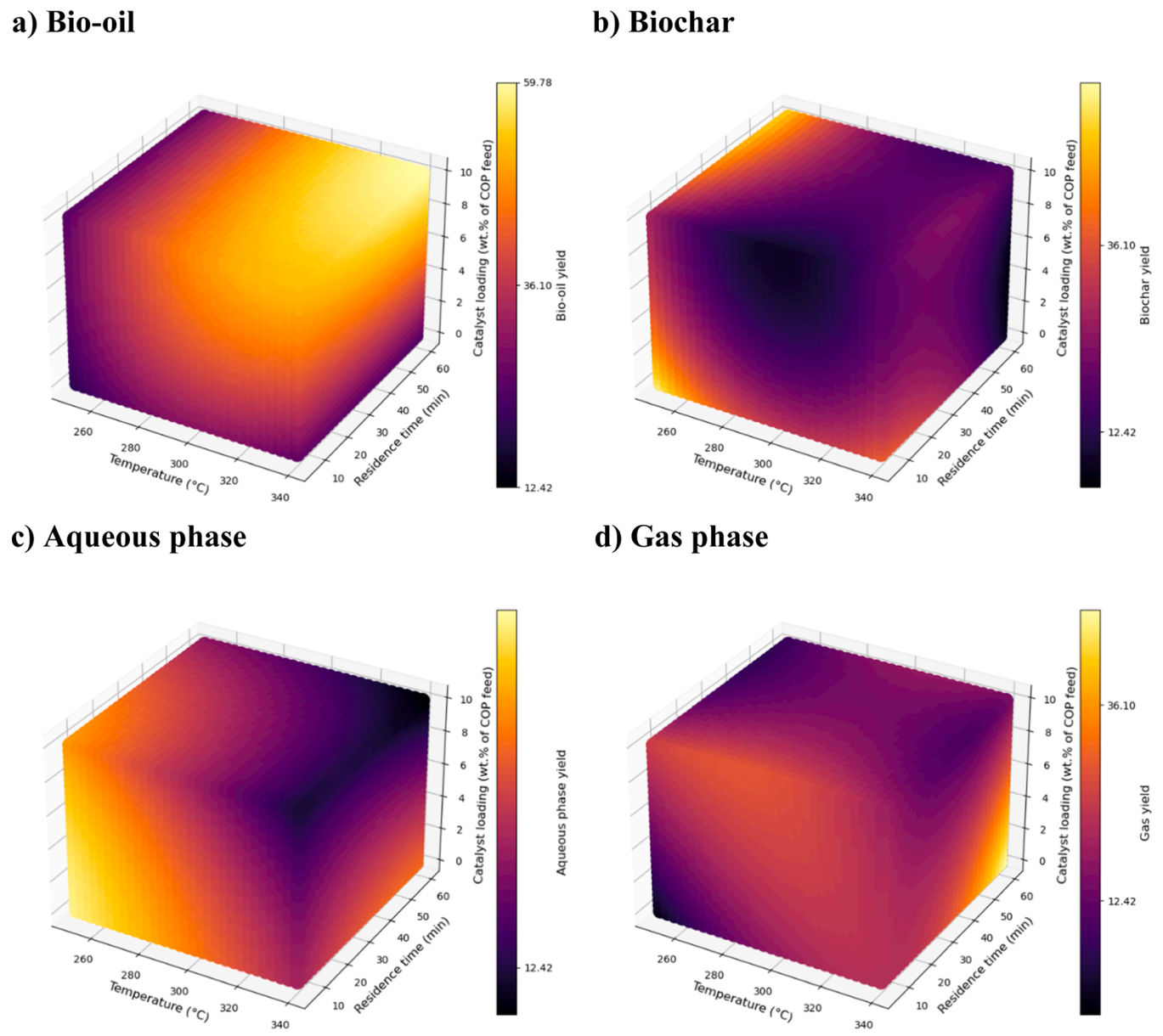

Fig. 6. Product distribution for COP HTL at different temperatures, residence time and catalyst loading.

Table 4
Quadratic models of bio-oil, biochar, aqueous phase and gas from the HTL of COP.

Bio-oil
−295.7 + 2.145 *X1–0.353 *Y1–4.19 *Y2–0.003531 *X1 * *2–0.00085 *Y1 * *2–0.1265 *Y2 * *2 + 0.00112 *X1 * Y1 + 0.02372 *X1 * Y2 + 0.0161 *Y1 *Y2
Biochar
676–4.21 *X1 + 1.54 *Y1–7.21 *Y2 + 0.00686 *X1 * *2–0.00681 *Y1 * *2 + 0.215 *Y2 * *2–0.00475 *X1 * Y1 + 0.0087 *X1 * Y2 + 0.0499 *Y1 *Y2
Aqueous phase
32.7 + 0.045 *X1–0.192 *Y1 + 0.71 *Y2–0.000265 *X1 * *2–0.001449 *Y1 * *2–0.0309 *Y2 * *2 + 0.001061 *X1 * Y1–0.00282 *X1 * Y2–0.0106 *Y1 *Y2
Gaseous phase
−311 + 2.01 *X1–1.00 *Y1 + 10.65 *Y2–0.00303 *X1 * *2 + 0.00925 *Y1 * *2–0.056 *Y2 * *2 + 0.00256 *X1 * Y1–0.0296 *X1 * Y2–0.0555 *Y1 *Y2

Where *X1* = Temperature (°C), *Y1* = residence time (min) and *Y2* = catalyst loading (wt%).

The condition that produced the highest gas phase yield was the one with the longest residence time (60 min), a temperature of 300°C and a catalyst loading of 5 wt%.

3.6. CCD campaign: energy recovery and elemental analysis of bio-oil, biochar and aqueous phase

The Energy Recovery (ER) ratio was used to illustrate the trade-off between the HHV and yield for bio-oil and biochar (Fig. 7) produced with and without catalyst. The five bio-oils from the CCD were selected in the following order: two with low bio-oil yields, one corresponding to

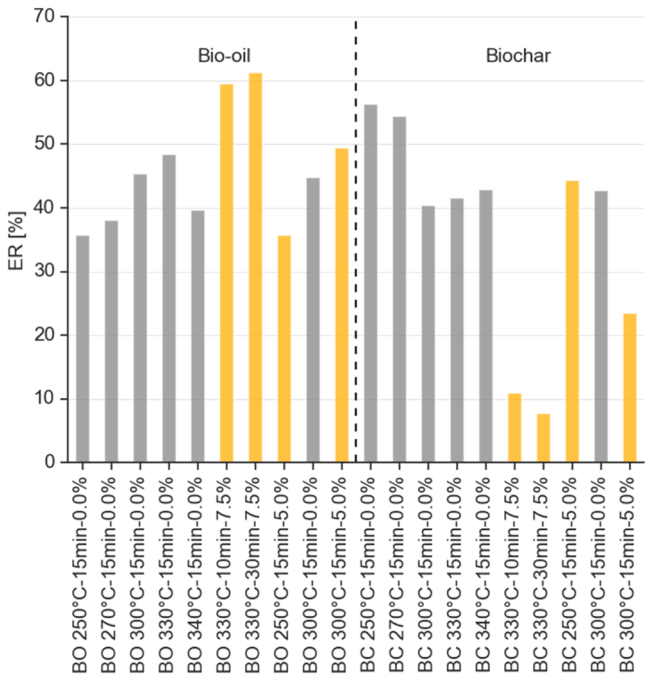

Fig. 7. Energy recovery (ER) for the non-catalytic campaign and for five of the selected bio-oils (BO) and biochars (BC) at different operational conditions. Non-catalytic samples are colored in gray and catalytic samples are colored in yellow.

central point of the CCD, and two with high bio-oil yields. The ER measures the proportion of the initial energy content of the feedstock that was converted into bio-oil or biochar. The energy recovery equation and HHV values can be found in the Supplementary information (Table S11).

As can be seen from Fig. 7, the use of the Ni/SiO_2-Al_2O_3 catalyst boosted the energy recovery compared to non-catalytic experiments, except for the low temperature catalytic experiment at 250°C, 15 min, and 5 wt%. This phenomenon is connected to the catalyst activity in hydrogenation processes [29]. The top-performing oils in terms of ER (> 59 %) are those produced at 300°C-30min-7.5 % and 300°C-10min-7.5 %. These oils contain more than half of the energy content of the feedstock. The results presented in Fig. 7 are encouraging because the ER of lignocellulosic biomass falls within the range of 23.6–57.6 % [30,31]. The HHVs for the five bio-oils from the CCD do not show a significant improvement in comparison to results from Dahdouh et al., [14] for HTL of Moroccan COP. However, our findings reveal a 35 % increase in the bio-oil yield (330°C-30min-7.5 %) compared to their best point (280°C_0.05 [14]). The catalyst's effects can also be seen during the 15-minute residence time tests. By using 5 wt% of the catalyst, the temperature was reduced by 30°C (300°C-15 min-5 %), resulting in a comparable ER to the non-catalytic experiment (330°C-15 min-0 %). Nonetheless, improving the ER for the bio-oils decreased the ER for the biochar.

The improvements in the ER are also correlated with the increase in carbon and hydrogen content in the bio-oils. Therefore, the Van Krevelen diagram is used to present the results of the ultimate analysis for five of the selected bio-oils and biochars for the CCD campaign (Fig. 8). The detailed ultimate and proximate analysis is provided in the Supplementary Information (Table S11 and Table S12).

As can be seen from Fig. 8, the O/C and H/C values for the bio-oils range between 0.31 and 0.46 and 1.35–1.77, respectively. The top-performing oils are 300°C-15min-0 % and 250°C-15min-5 %, which have low aromatization based on their H/C values. On average, the Ni/SiO_2-Al_2O_3 catalyst generated bio-oils with a 32 % oxygen content, while the non-catalytic bio-oils from Dahdouh et al. [14] had a 22 % oxygen content, and the non-catalytic and catalytic bio-oils reported by Evcil et al. [12] had a 24 % oxygen content. The presence of the Ni/SiO_2-Al_2O_3 catalyst had a significant impact on the production of oxygenated compounds, leading to a decrease in the HHV compared to the non-catalytic experiments (Table S11). Furthermore, the bio-oils consistently exhibited a lower concentration of N compared to the

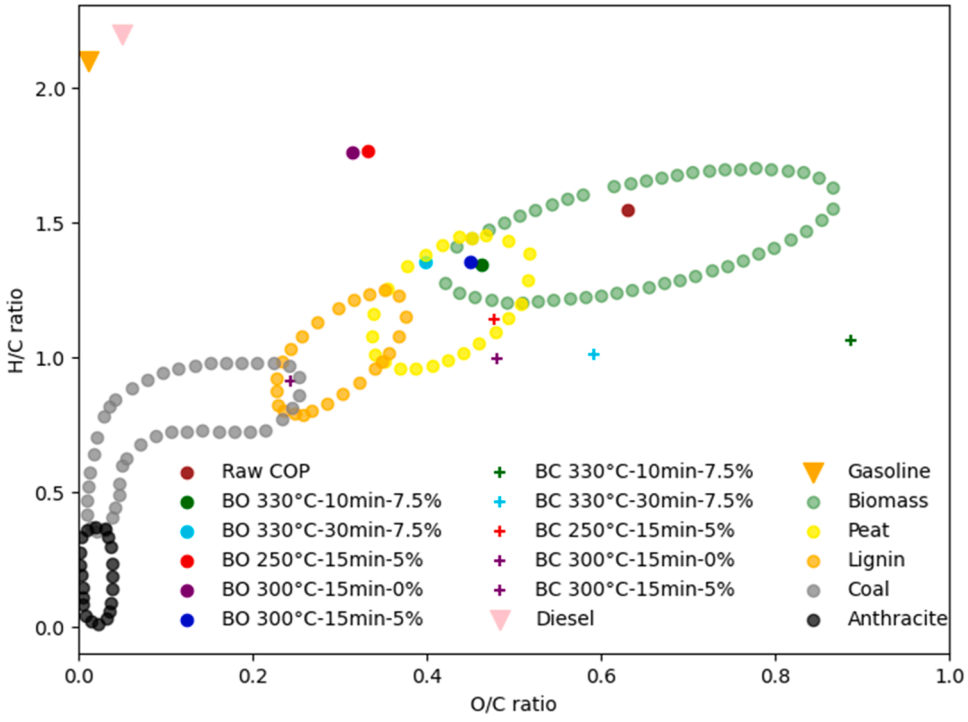

Fig. 8. Van Krevelen diagram for five of the selected bio-oils and biochars for the CCD. The bio-oils are represented by coloured circles, while the biochars by coloured crosses.

parent feedstock.

With respect to the biochar, the O/C and H/C values range from 0.24 to 0.88 and 0.91–1.14, respectively. In this sense, a higher concentration of catalyst (7.5 wt%) led to the production of biochars with less ER (Fig. 7) and higher ash content (≈ 41 %, Table S12). Thus, the only biochars that have potential as solid fuel are the ones produced at 250°C-15min-5 % and 300°C-15min-0 %. These findings are consistent with the results of the ICP-OES analysis, indicating that, on average, 98 % of Ni and 92 % of Si were found in the biochar (Fig. 9 and Table S13), suggesting minimal dissolution/degradation of the Ni/SiO_2-Al_2O_3 catalyst during HTL.

Significant quantities of Cl, K and Ca migrated to the aqueous phases. The Cl content in aqueous phases is attributed to the aqua regia used to dissolve the samples for ICP-OES analysis. Additionally, the traces of Cr, Cu, Mo and Mn are attributed to the reactor's alloy [9]. Furthermore, the COD of the aqueous phases (Table S14) ranges between 89 and 364 g/l. The observed COD range is relatively large for aqueous phases derived from HTL of lignocellulosic biomass [32]. This suggests that a significant fraction of the organic carbon originally present in the COP became water soluble during HTL.

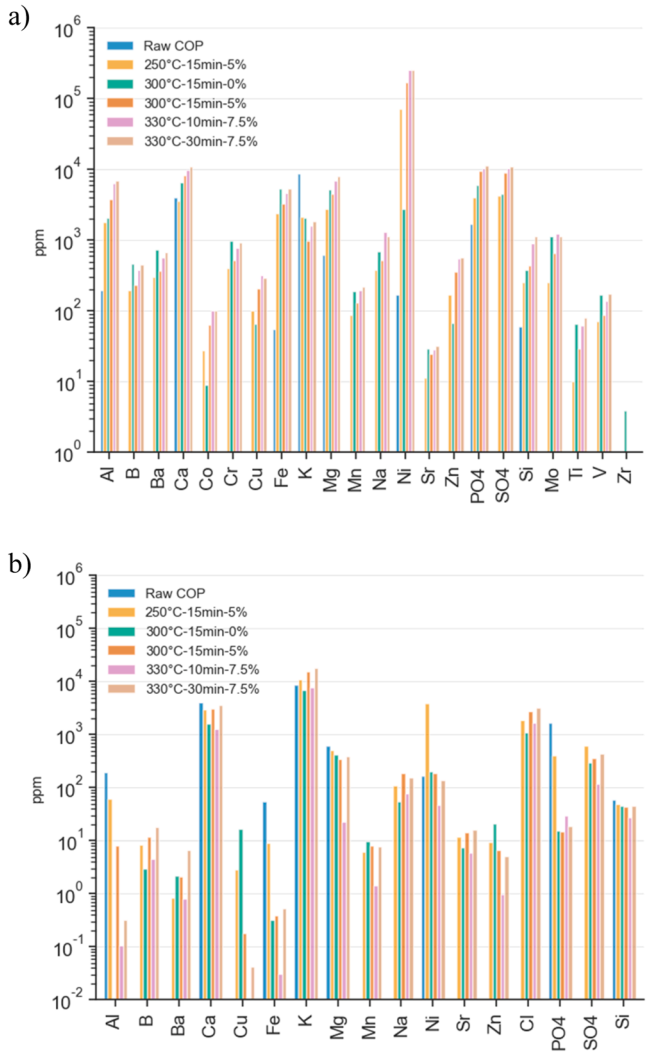

Fig. 9. ICP-OES for five of the selected biochars and aqueous phases at different operational conditions. a) ICP-OES for five of the selected biochars of the CCD. b) ICP-OES for five of the selected aqueous phases of the CCD.

3.7. CCD campaign: bio-oil chemical composition by GC-MS

In order to determine the chemical composition in each of the five selected bio-oils, GC-MS analysis was performed. Chromatograms showing the percentage area of each bio-oil are shown in Fig. 10. The detailed list of compounds detected in each bio-oil by GC-MS is available in the Supplementary Information Table S15-S19.

Phenols were the most prominent functional group found in the studied bio-oils, while ketones, alkenes, and carboxylic acids were also detected (Fig. 10). Two of the most important phenolic compounds found in the bio-oils were guaiacol (2-methoxy phenol) and syringol (2,6-dimethoxyphenol). This is consistent with previous observations described in literature [14]. Syringol yields dropped with higher temperature and extended residence times in bio-oils at 330°C-10min-7.5 % and 330°C-30min-7.5 %, while creosol became relevant. When comparing to the non-catalytic point at 300°C-15min-0 %, these oils showed an increase in phenol content by an average of 20 % and a decrease in alkenes by 70 %.

All samples also contained Octadecanoic acid and n-Hexadecanoic acid, which is consistent with the findings reported by Dahdouh et al. [14]. In this regard, the higher the temperature, residence time, and catalyst loading, the higher the content of phenolic compounds as well as carboxylic acids. The bio-oils with the highest carboxylic acid groups are 330°C-10min-7.5 % and 330°C-30min-7.5 %. These bio-oils had lower HHVs compared to other samples (Table S11), likely due to the presence of an oxygen-containing functional group in carboxylic acids.

The principal component analysis (PCA), illustrated in Fig. 11, is used to identify the variables that most significantly impacted the distribution of HTL bio-crude oils among the five samples.

As can be seen from Fig. 11, the first two principal components accounted together for 76.7 % of the total variance. In PC1, alcohols, esters and phenones represent 54.80 % of the total variance, while PC2 is described by carboxylic acids, with 21.89 % of the total variance. In addition, Fig. 11 provides confirmation that all bio-crude oils have a significant presence of phenols, particularly BO-330–30–7.5 followed by BO-300–15–5.0. On the other hand, BO-300–15–0.0 is characterized by its high concentration of carboxylic acids. In addition, there is a strong relationship between nitrogen-containing compounds and fatty acids, as well as between esters and alcohols. Nitrogen-containing molecules

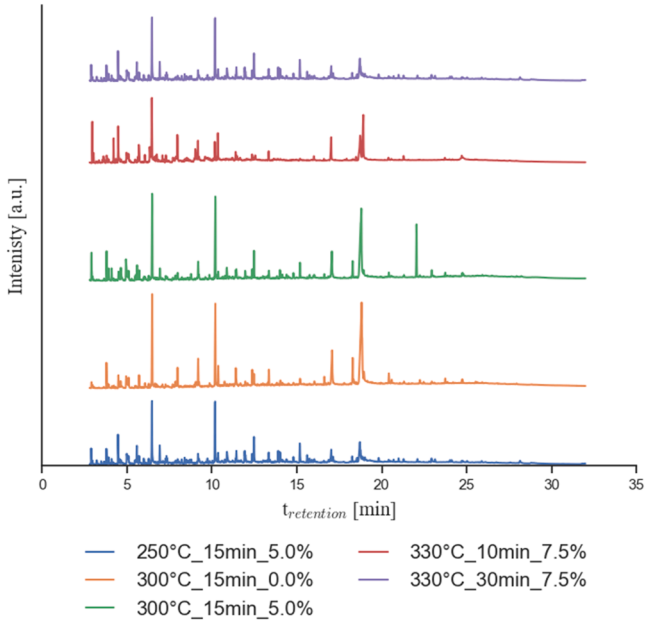

Fig. 10. GC-MS analysis for five of the selected bio-oils of the CCD at different operational conditions.

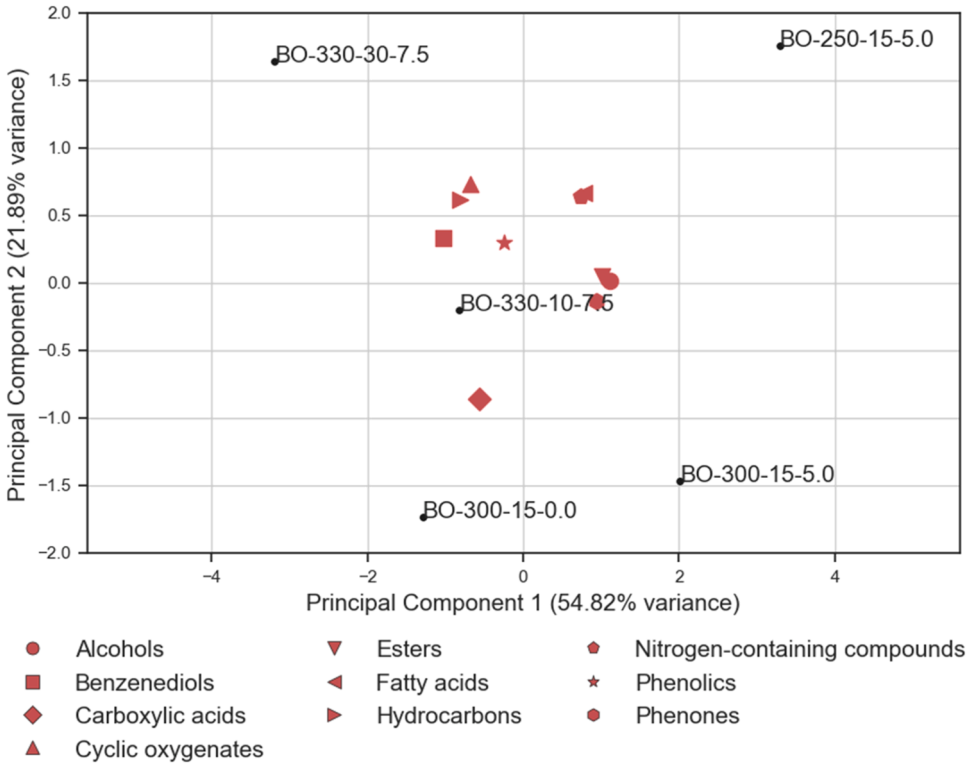

Fig. 11. Principal Component Analysis (PCA) and loadings for five of the selected bio-oils of the CCD at different operational conditions.

were found in lower concentrations, but their concentration increased when Ni/SiO_2-Al_2O_3 catalyst was used compared to the non-catalytic sample.

3.8. Kinetic model and parameter estimation

Fig. 12 presents the results of the kinetic model (KM) presented in Fig. 2, ODEs system and experimental values for 250°C, 300°C and 340°C with a 5 wt% catalyst loading. The KM is shown using dashed lines, the numerical solution of the ODEs system is represented by a continuous line, and the RSM evaluations at different times are represented with circular markers. The discrete points (triangles) are the experimental values from the CCD campaign. In addition, Table 5 presents the optimized rate constants of each reaction pathway during the HTL of COP, as well as the corresponding activation energies (E_a).

According to the KM results, biochar is the main product at low temperatures (250°C), whereas bio-oil becomes the dominating product at higher temperatures (250°C and 340°C). At higher temperatures, the conversion of the feedstock into AP components and bio-oil was more noticeable and occurred more rapidly that the formation of solid residue (biochar). This is confirmed by the kinetic constants k_1 and k_2 which are 125 % larger than k_3. In all cases represented by the KM, there is a clear competition between the aqueous phase and the bio-oil. Results from the KM (Table 5) indicate that at higher temperatures, the conversion of AP→Bio-oil (k_4) is more favorable than the conversion of Bio-oil→AP (k_5), whereas bio-oil→SR (k_6), AP→gas (k_7) and bio-oil→gas (k_8) are less favorable due to their small reaction rate constants. However, large negative activation energies are needed to fit the experimental results (Table 5), especially for steps involving k_3 to k_6 and k_8, indicating that the reaction rate decreases with increasing temperature. These reactions are often called barrier-less reactions because they depend on molecules being captured for the reaction to happen [33,34].

In addition, the KM results shows that the production of bio-oil reaches its maximum value at $t < 10$ min, while the RSM results suggests that this only occurs at $t \approx 30$ min, except for temperatures around 340°C. It is therefore verified that the KM (Fig. 12) does not match the experimental values obtained during the CCD campaign. This is particularly pronounced for Fig. 12 at 340°C, where the KM overestimates the biochar yield and underestimates the gas phase (Fig. 12-c). The differences between the global KM and experimental results have been previously discussed by [16].

On the other hand, the overlap of the RSM values with the ODE system results validates the accuracy of the analytical derivation of the ODE coefficients. As an example, the ODE system that was found for 270°C and 2.5 % C is:

$$\frac{dY_{oil}}{dt} = 0.018Y_{oil} - 0.015Y_{SR} + 0.001Y_{AP} - 0.009Y_{gas}$$

$$\frac{dY_{SR}}{dt} = 0.148Y_{oil} - 0.114Y_{SR} + 0.010Y_{AP} - 0.068Y_{gas}$$

$$\frac{dY_{AP}}{dt} = 0.031Y_{oil} - 0.024Y_{SR} + 0.002Y_{AP} - 0.015Y_{gas}$$

$$\frac{dY_{gas}}{dt} = -0.200Y_{oil} + 0.155Y_{SR} - 0.013Y_{AP} + 0.094Y_{gas}$$

A drawback of using the RSM to find the ODEs system is that the resulting system's accuracy is limited to the quadratic response function from the CCD models and restricts the generation of kinetic data such as rate constants and activation energies. Additionally, the coefficients matrix C is not unique due to the system overdetermination. In future research, it is recommended to use a cubic function as the RSM when working with a larger number of experimental samples. This will result in a well-defined system due to the inclusion of an additional term in the cubic expression.

4. Conclusions

The results indicate that HTL of COP can achieve significant yields of bio-oil, 51.96 wt%, when using a Ni/SiO_2-Al_2O_3 catalyst. Furthermore,

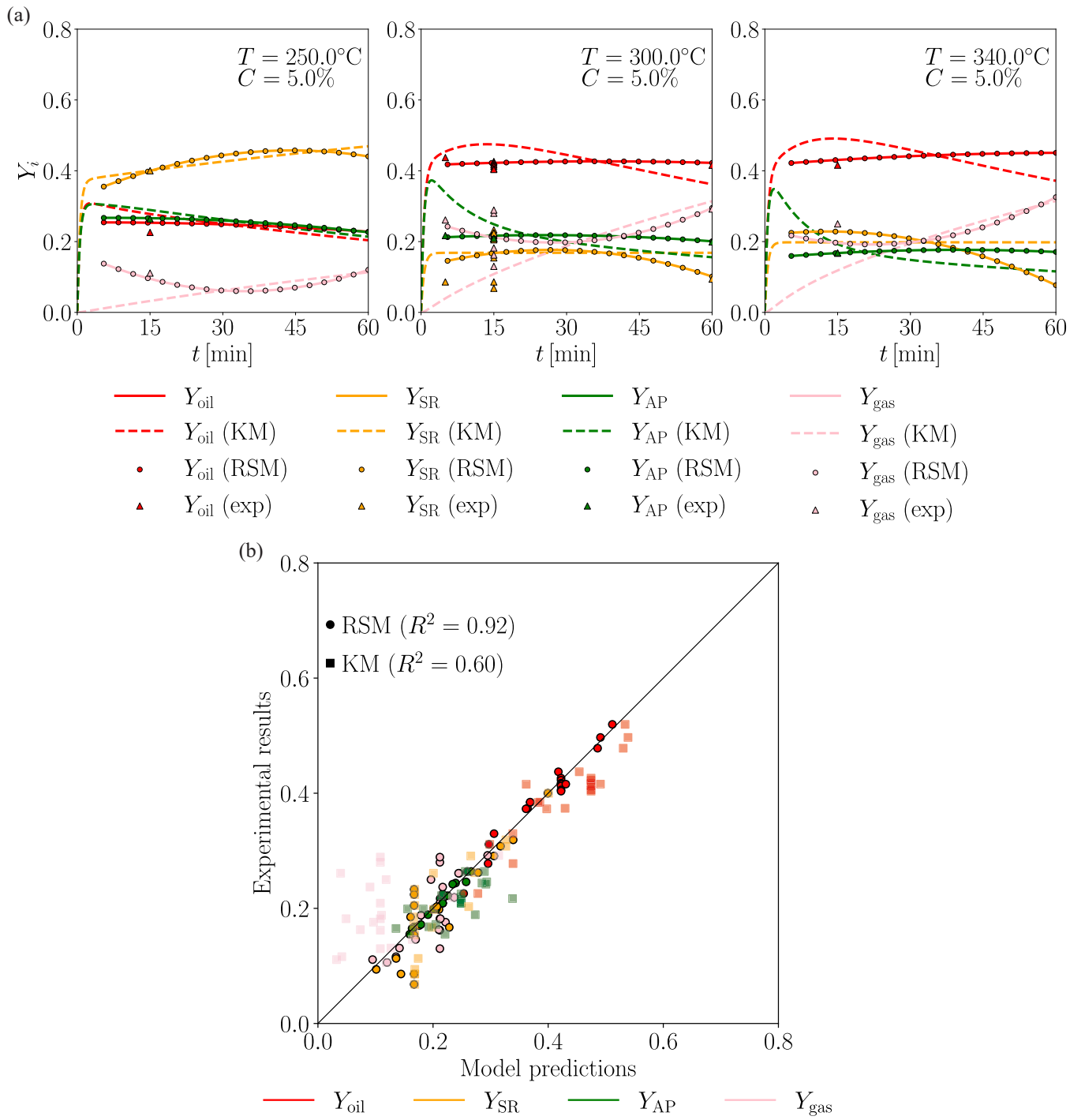

Fig. 12. Kinetic model results for COP HTL. a) Kinetic model results, ODEs system and experimental values (discrete points) for HTL of COP at 250°C, 300°C and 340°C for a catalyst loading of 5 wt%. The kinetic model (KM) is represented with dashed lines. The continuous line with circular markers represents the numerical solution of the ODEs system, which was obtained using a Runge-Kutta 4th-order method. The discrete points (triangles) are the experimental values from the CCD campaign. b) Comparison of the HTL product yields provided by the kinetic model (KM) and the numerical solution of the ODEs system for the CCD response surface model (RSM).

using the Ni/SiO_2-Al_2O_3 catalyst resulted in higher phenol and carboxylic acid content in the bio-oils, as opposed to the non-catalytic experiments. When using the catalyst, there are trade-offs between energy content and the bio-oil output. Nevertheless, the efficiency of the ER increased by 60 % when 7.5 wt% catalyst was utilized, in comparison to cases when no catalyst was present. Results from a global kinetic model suggest that the conversion of COP into aqueous phase and bio-oil was more prominent and occurred at a faster rate compared to the formation of biochar at higher temperatures. Nonetheless, a linear system of ODEs (R^2= 0.92) predicted HTL product yields more accurately than the global kinetic model (R^2= 0.60).

CRediT authorship contribution statement

de Jong Wiebren: Writing – review & editing, Supervision, Methodology, Conceptualization. **Font Bernat:** Writing – review & editing,

Table 5
Optimized kinetic rate constants and activation energies for COP HTL for reaction network presented in Fig. 2.

Paths	Rate constant (min^{-1})			E_a (kJ/mol)
	250°C	300°C	340°C	
k_1: COP→AP	0.577	0.700	0.700	6.003
k_2: COP→Bio-oil	0.598	0.700	0.700	4.914
k_3: COP→SR	0.700	0.283	0.346	−22.708
k_4: AP→Bio-oil	0.081	0.064	0.079	−1.658
k_5: Bio-oil→AP	0.078	0.035	0.032	−27.584
k_6: Bio-oil→SR	0.006	1.38E−26	9.24E−22	−1391.162
k_7: AP→Gas	4.45E−26	0.024	0.031	1707.604
k_8: Bio-oil→Gas	0.008	1.24E−26	1.96E−24	−1565.701

Formal analysis. **Al-Naji Majd:** Investigation, Formal analysis. **Cutz Luis:** Writing – review & editing, Writing – original draft, Methodology, Investigation, Formal analysis, Conceptualization. **Misar Sarvesh:** Methodology, Investigation, Formal analysis.

Declaration of Competing Interest

The authors declare that they have no known competing financial interests or personal relationships that could have appeared to influence the work reported in this paper.

Acknowledgements

This work was supported by the Dutch Research Council (NWO) in the context of the 'Value from Biomass' programme, "Clean Shipping", Biom.2019.002. We would like to thank Ruud Hendrikx for conducting the XRD and XRF analyses at the Materials Science and Engineering Department of the Delft University of Technology. Finally, we thank Ing. Michel van den Brink from the Process & Energy Department of the Delft University of Technology for providing technical support during the execution of this project.

Appendix A. Supporting information

Supplementary data associated with this article can be found in the online version at doi:10.1016/j.jaap.2025.107050.

Data availability

Data will be made available on request.

References

[1] P. de Filippis, B. de Caprariis, M. Scarsella, A. Petrullo, N. Verdone, Biocrude production by hydrothermal liquefaction of olive residue, Int. J. SDP 11 (2016) 700–707, https://doi.org/10.2495/SDP-V11-N5-700-707.
[2] J.F. García Martín, M. Cuevas, C.-H. Feng, P. Álvarez Mateos, M. Torres García, S. Sánchez, Energetic valorisation of olive biomass: olive-tree pruning, olive stones and pomaces, Processes 8 (2020) 511, https://doi.org/10.3390/pr8050511.
[3] N. Kalogeropoulos, A.C. Kaliora, A. Artemiou, I. Giogios, Composition, volatile profiles and functional properties of virgin olive oils produced by two-phase vs three-phase centrifugal decanters, LWT - Food Sci. Technol. 58 (2014) 272–279, https://doi.org/10.1016/j.lwt.2014.02.052.
[4] I. Miranda, R. Simões, B. Medeiros, K.M. Nampoothiri, R.K. Sukumaran, D. Rajan, H. Pereira, S. Ferreira-Dias, Valorization of lignocellulosic residues from the olive oil industry by production of lignin, glucose and functional sugars, Bioresour. Technol. 292 (2019) 121936, https://doi.org/10.1016/j.biortech.2019.121936.
[5] T.B. Ribeiro, A.L. Oliveira, C. Costa, J. Nunes, A.A. Vicente, M. Pintado, Total and Sustainable Valorisation of Olive Pomace Using a Fractionation Approach, Appl. Sci. 10 (2020) 6785, https://doi.org/10.3390/app10196785.
[6] M. Orive, M. Cebrián, J. Amayra, J. Zufía, C. Bald, Integrated biorefinery process for olive pomace valorisation, Biomass-.-. Bioenergy 149 (2021) 106079, https://doi.org/10.1016/j.biombioe.2021.106079.
[7] D. Castello, T.H. Pedersen, L.A. Rosendahl, Continuous hydrothermal liquefaction of biomass: a critical review, Energies 11 (2018) 3165, https://doi.org/10.3390/en11113165.
[8] M. Usman, S. Cheng, S. Boonyubol, J.S. Cross, From biomass to biocrude: innovations in hydrothermal liquefaction and upgrading, Energy Convers. Manag. 302 (2024) 118093, https://doi.org/10.1016/j.enconman.2024.118093.
[9] L. Cutz, H. Maldonado, G. Zambrano, M. Al-Naji, W. de Jong, Hydrothermal liquefaction of Elaeis guineensis trunks: Lessons learned from a case study in Guatemala, Ind. Crops Prod. 206 (2023) 117552, https://doi.org/10.1016/j.indcrop.2023.117552.
[10] L. Cutz, N. Bias, M. Al-Naji, W. de Jong, Exploring the catalytic hydrothermal liquefaction of Namibian encroacher bush, Sci. Rep. 15 (2025) 112, https://doi.org/10.1038/s41598-024-83881-8.
[11] D.C. Elliott, P. Biller, A.B. Ross, A.J. Schmidt, S.B. Jones, Hydrothermal liquefaction of biomass: Developments from batch to continuous process, Bioresour. Technol. 178 (2015) 147–156, https://doi.org/10.1016/j.biortech.2014.09.132.
[12] T. Evcil, K. Tekin, S. Ucar, S. Karagoz, Hydrothermal liquefaction of olive oil residues, Sustain. Chem. Pharm. 22 (2021) 100476, https://doi.org/10.1016/j.scp.2021.100476.
[13] B. Cantero-Tubilla, D.A. Cantero, C.M. Martinez, J.W. Tester, L.P. Walker, R. Posmanik, Characterization of the solid products from hydrothermal liquefaction of waste feedstocks from food and agricultural industries, J. Supercrit. Fluids 133 (2018) 665–673, https://doi.org/10.1016/j.supflu.2017.07.009.
[14] A. Dahdouh, Y. Le Brech, I. Khay, A. El Maakoul, M. Bakhouya, Hydrothermal liquefaction of Moroccan two-phase olive mill waste (alperujo): Parametric study and products characterizations, Ind. Crops Prod. 205 (2023) 117519, https://doi.org/10.1016/j.indcrop.2023.117519.
[15] Z. Zhu, L. Rosendahl, S.S. Toor, G. Chen, Optimizing the conditions for hydrothermal liquefaction of barley straw for bio-crude oil production using response surface methodology, Sci. Total Environ. 630 (2018) 560–569, https://doi.org/10.1016/j.scitotenv.2018.02.194.
[16] H. Wang, X. Han, Y. Zeng, C.C. Xu, Development of a global kinetic model based on chemical compositions of lignocellulosic biomass for predicting product yields from hydrothermal liquefaction, Renew. Energy 215 (2023) 118956, https://doi.org/10.1016/j.renene.2023.118956.
[17] A. Sluiter, Hames, D. Hyman, C. Payne, P. Ruiz, C. Scarlata, J. Sluiter, D. Templeton, J. Wolfe, Determination of Total Solids in Biomass and Total Dissolved Solids in Liquid Process Samples, NREL, 2008.
[18] A. Sluiter, Hames, P. Ruiz, C. Scarlata, J. Sluiter, Determination of ash in biomass, NREL, 2008.
[19] M. Del Grosso, L. Cutz, U. Tiringer, C. Tsekos, P. Taheri, W. de Jong, Influence of indirectly heated steam-blown gasification process conditions on biochar physico-chemical properties, Fuel Process. Technol. 235 (2022) 107347, https://doi.org/10.1016/j.fuproc.2022.107347.
[20] F. Brandi, B. Pandalone, M. Al-Naji, Flow-through reductive catalytic fractionation of beech wood sawdust, RSC Sustain (2023), https://doi.org/10.1039/D2SU00076H.
[21] A.-L. Skaltsounis, A. Argyropoulou, N. Aligiannis, N. Xynos, Recovery of High Added Value Compounds from Olive Tree Products and Olive Processing Byproducts, in: D. Boskou (Ed.), Olive and Olive Oil Bioactive Constituents, 11, AOCS Press, 2015, pp. 333–356, https://doi.org/10.1016/B978-1-63067-041-2.50017-3.
[22] P. Leite, J. Salgado, L. Abrunhosa, A. Venâncio, I. Belo, Sonication of olive pomace to improve xylanases production by SSF, in: WASTES 2015 – Solutions, Treatments and Opportunities, 2015: pp. 127–132. ⟨https://doi.org/10.1201/b18853-23⟩.
[23] C. Steiner, A.O. Bayode, T.K. Ralebitso-Senior, Chapter 2 - Feedstock and Production Parameters: Effects on Biochar Properties and Microbial Communities, in: T.K. Ralebitso-Senior, C.H. Orr (Eds.), Biochar Application, Elsevier, 2016, pp. 41–54, https://doi.org/10.1016/B978-0-12-803433-0.00002-3.
[24] M.K. Akalin, K. Tekin, S. Karagöz, Hydrothermal liquefaction of cornelian cherry stones for bio-oil production, Bioresour. Technol. 110 (2012) 682–687, https://doi.org/10.1016/j.biortech.2012.01.136.
[25] T. Evcil, K. Tekin, S. Ucar, S. Karagoz, Hydrothermal liquefaction of olive oil residues, Sustain. Chem. Pharm. 22 (2021), https://doi.org/10.1016/j.scp.2021.100476.
[26] M. Attya, H. Benabdelkamel, E. Perri, A. Russo, G. Sindona, Effects of Conventional Heating on the Stability of Major Olive Oil Phenolic Compounds by Tandem Mass Spectrometry and Isotope Dilution Assay, Molecules 15 (2010) 8734–8746, https://doi.org/10.3390/molecules15128734.
[27] M. Antónia Nunes, A.S.G. Costa, S. Bessada, J. Santos, H. Puga, R.C. Alves, V. Freitas, M.B.P.P. Oliveira, Olive pomace as a valuable source of bioactive compounds: a study regarding its lipid- and water-soluble components, Sci. Total Environ. 644 (2018) 229–236, https://doi.org/10.1016/j.scitotenv.2018.06.350.
[28] B. de Caprariis, M. Scarsella, I. Bavasso, M.P. Bracciale, L. Tai, P. De Filippis, Effect of Ni, Zn and Fe on hydrothermal liquefaction of cellulose: impact on bio-crude yield and composition, J. Anal. Appl. Pyrolysis 157 (2021) 105225, https://doi.org/10.1016/j.jaap.2021.105225.
[29] M. Scarsella, B. de Caprariis, M. Damizia, P. De Filippis, Heterogeneous catalysts for hydrothermal liquefaction of lignocellulosic biomass: a review, Biomass-.-. Bioenergy 140 (2020) 105662, https://doi.org/10.1016/j.biombioe.2020.105662.
[30] L. Nazari, Z. Yuan, S. Souzanchi, M.B. Ray, C. (Charles) Xu, Hydrothermal liquefaction of woody biomass in hot-compressed water: Catalyst screening and comprehensive characterization of bio-crude oils, Fuel 162 (2015) 74–83, https://doi.org/10.1016/j.fuel.2015.08.055.
[31] T.H. Seehar, S.S. Toor, K. Sharma, A.H. Nielsen, T.H. Pedersen, L.A. Rosendahl, Influence of process conditions on hydrothermal liquefaction of eucalyptus biomass for biocrude production and investigation of the inorganics distribution,

Sustain. Energy Fuels 5 (2021) 1477–1487, https://doi.org/10.1039/D0SE01634A.
[32] Z. Bi, J. Zhang, E. Peterson, Z. Zhu, C. Xia, Y. Liang, T. Wiltowski, Biocrude from pretreated sorghum bagasse through catalytic hydrothermal liquefaction, Fuel 188 (2017) 112–120, https://doi.org/10.1016/j.fuel.2016.10.039.
[33] P. Parthasarathy, S.K. Narayanan, Determination of kinetic parameters of biomass samples using thermogravimetric analysis, Environ. Prog. Sustain. Energy 33 (2014) 256–266, https://doi.org/10.1002/ep.11763.
[34] S.B. Prajapati, A. Gautam, S. Gautam, Z. Yao, F. Tesfaye, X. Lü, Co-pyrolysis behavior, kinetic and mechanism of waste-printed circuit board with biomass, Processes 11 (2023) 229, https://doi.org/10.3390/pr11010229.